Fabrication and Electrical Characterization of AlGaN/GaN HFETs

[1]Michael A. Awaah, [2]Isibhakhomen Awaah, [2]Okechukwu Akpa, [3]Uwadiae Obahiagbon and [4]Vitus A. Apalangya
[1]Faculty Member, CHSS Grand Canyon University, 3300 W. Camelback Road Phoenix AZ 85017 USA
[2] Senior Process Engineer, 3320 E Yellowstone Place, Chandler Arizona 85249 USA
[3] Graduate Student, Electrical Engineering Dept., Arizona State University. Tempe, AZ, 85281 USA
[4] Lecturer, Dept. of Food Process Engineering, School of Engineering, University of Ghana, Legon, Ghana

Received: 11.15.2016/ Accepted: 11.23.2016

Abstract: Ni/AlGaN/GaN rectifying diodes test structure was fabricated, representative of the gate element of heterostructure FET (HFETs) with annealed ohmic "back contacts" and HFET devices of various geometries. Electrical measurements on TLM pads test produced a contact resistivity of 2.0×10^{-3} Ω.cm^2, a barrier height of ~1.1 eV for the rectifying diodes, a sheet charge density of ~1.1×10^{13} cm^{-2} at the AlGaN/GaN interface, and a conduction band offset of 0.27 eV. These values are in close agreement with those reported by other researchers. The HEMT devices yielded a drift mobility of ~511 cm^2/s and a transconductance of 10 – 25 mS.

Keywords: GaN HEMTs, GaN HFETs AlGaN HEMTs, AlGaN HFETs, HEMT devices, Transconductance, Drift Mobility, Contacts

I. INTRODUCTION

Gallium nitride (GaN) possesses several outstanding physical properties, which make it particularly attractive for solid-state device applications. In particular, the GaN based material system is of great interest for blue/green light-emitting diodes (LEDs), laser diodes, UV photodetectors, and also for the realization of high frequency and high-power electronic devices for operation at elevated temperatures. As a wide direct bandgap material ($E_g \approx 3.4$ eV), GaN has a very high breakdown field (approximately 3 MV/cm) [1, 2], high saturation velocity, ($\approx 2\times 10^7$ cm/s), and high sheet charge concentration in the AlGaN/GaN interface. The high breakdown field allows GaN-based devices to be biased at very high drain voltages ($V_{break\text{-}down}$ = 50 – 500 V) depending on the application of the device. The high saturation electron velocity contributes to a higher current density since, $I_{\max} \propto q n_s \upsilon_s$, where q is the electronic charge, n_s is the sheet charge density, υ_s is the electron saturation velocity, and also a high operating frequency, since $f_t \propto \upsilon_s / L_{eff}$.

The existence of the AlGaN/GaN heterostructure leads to a high sheet charge density ($n_s = 1\times 10^{13}$ /cm^2), which contributes to a high $I_{\max}$; whereas the high electron mobility ($\mu = 1200 - 1500$ cm^2/V.s) contributes to a low on-resistance, since channel resistance is related to $1/qn_s\mu E$ at low electric fields. These physical properties of GaN translate into fundamental performance advances in the area of high power, high frequency power transistors for RF applications covering over a 75 GHz band.

Group-III nitrides exhibit fairly high bond strength and very high melting temperatures. The large bond strength could possibly inhibit dislocation motion and improve reliability in comparison to other II-VI and III-V materials [3]. In addition, the nitrides are resistant to chemical etching and should allow GaN-based devices to be operated under harsh environments.

An ideal heterojunction consists of a semiconductor crystal in which there exists a plane across which the identity of the atoms constituting the crystal changes abruptly. In reality, the ideal structure is approached quite closely in some systems such as molecular beam epitaxy (MBE) grown $Al_xGa_{1-x}As/GaAs$ heterojunctions with essentially atomically abrupt interfaces [3, 4].

In the reported work, isotype heterojunctions between unintentionally doped n-type AlGaN and GaN are considered. When two n-type semiconductors with different bandgaps and work functions are brought into contact, in order to establish an equilibrium, electrons flow from the wider to the narrower bandgap material resulting in an alignment of the Fermi levels with associated band bending and band discontinuity, as indicated in Figure 1. These electrons accumulate in a narrow region of lowest energy – a quantum well – at the interface between the two semiconductors forming a "sheet" of charge, generally referred to as two-dimensional electron gas (2DEG). Electrons in the 2DEG exhibit much higher mobility than the bulk material forming the heterostructure as they are physically separated from the donors in the material causing minimal impurity scattering.

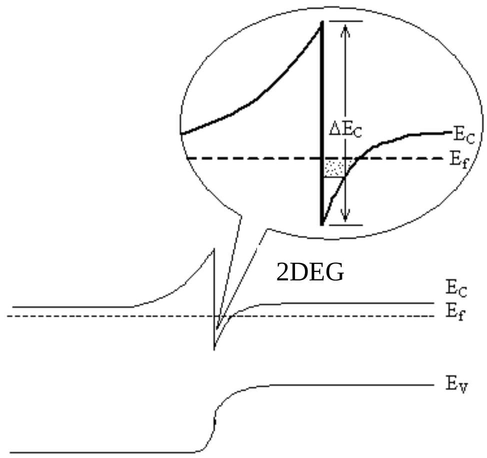

Figure 1. Band discontinuity in a unipolar heterostructure

The sheet charge density at the AlGaN/GaN interface is further enhanced due to spontaneous polarization arising from the asymmetry existing in the AlGaN and GaN crystal structure and also by piezoelectric polarization due to strain at the heterointerface [4]. The total charge at the AlGaN/GaN interface can exceed 1×10^{13} cm^{-2}, which is roughly five times higher than the AlGaAs/GaAs heterostructure. This high density 2DEG in the AlGaN/GaN system has been successfully employed as the conducting channel in the fabrication of a class of high performance field effect transistors, commonly referred to as high electron mobility transistors (HEMTs) [5-9].

II. METHODOLOGY

Test structures were fabricated using two sets of photo masks. The first, a set of three masks for the fabrication of Ohmic and rectifying contacts, the second set, a set of five masks designed as a part of the present study, was used for the fabrication of HFET devices. The fabricated devices on the heterostructures were electrically characterized.

For the study of ohmic contacts, rectangular pads measuring 100 μm × 400 μm with unequal spacing (3 μm, 5 μm, 10 μm, 15 μm, 20 μm, 25 μm, 30 μm, 35 μm, 40 μm, 45 μm) between contacts were used, as shown in Figure 2. This enabled the measurement of the resistivity using the transfer length method (TLM). Contact resistivity was obtained from plots of measured resistance between two adjacent pads as a function of pad separation.

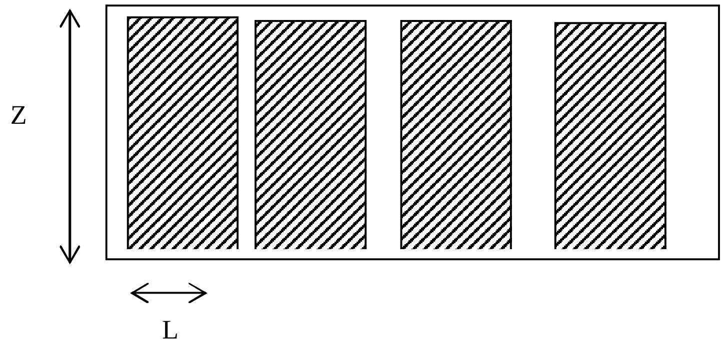

Figure 2. A schematic diagram of TLM contact pads used for the measurement of the contact resistance

Schottky contacts used for the study of rectifying characteristics consist of two set of circular contacts of varying diameters (set 1: 100, 200, 300 and 400 and set2: 150, 250 and 350 μm) surrounded by 15 and 25 μm wide ring-shaped ohmic contacts with probing pads. The first mask defines the ring-shaped ohmic contacts. The second mask defines circular Schottky contacts within the area bounded by the ring-shaped ohmic contacts. The third mask defined the contact pads. Additional thickness of Au was deposited on the contact pads.

The samples used for this research were MBE grown material obtained from SVT Associates, Eden Prairie, Minnesota. The heteroepitaxial film of $Al_{0.2}Ga_{0.8}N$/GaN on sapphire consisted of 20 nm unintentionally doped $Al_{0.2}Ga_{0.8}N$ grown on 1 μm unintentionally doped GaN, with donor concentration of $\approx 1\times10^{15}$ cm^{-3} [10]. As grown GaN film show n-type characteristics. Native point defects and nitrogen vacancies are thought to be primarily responsible for the n-type characteristic of the as grown films. The 2"diameter wafers were diced into 5 mm × 5 mm samples by the vendor. The as-received samples were cleaned in acetone and methanol and rinsed in deionized (DI) water. This removed organic contaminants from the sample. Samples were then treated in a buffered oxide etchant (BOE) solution for 5 min. to remove oxide film that might have been present on the surface of the sample.

A multi-layer Ti/Al/Ni/Au (15/60/35/50 nm) metallization was chosen for ohmic contact. This multi-layer metallization was chosen in order to obtain low specific contact resistivity, good surface adhesion and long life-time [11]. Schottky contact was defined by lift-off of Ni/Au (20/180 nm). Device fabrication was completed with a deposition of a passivation layer. The Ti layer was deposited to help in the formation of n^+ - GaN interface and provide a good adherence to the surface. Au layer was for preventing the oxidation of the Al and a better conductivity of the metal layers, and Ni layer was utilized for reducing of the Au/Al intermixing.

III. RESULTS AND DISCUSSION

From resistance measurement using TLM pads, contact resistivity of ohmic contacts and sheet resistivity of the AlGaN/GaN film were determined. The barrier height of the rectifying Ni/AlGaN/GaN contact was determined from I-V and C-V measurement. Capacitance-voltage measurements were also used to determine conduction band discontinuity, polarization charge and sheet charge density and the carrier concentration profile at the AlGaN/GaN interface. Device parameters such as transconductance and drift mobility were extracted from the measurement on the AlGaN/GaN fat FET devices.

Multi-layer TiAlNiAu contacts in the as-deposited state were semi-ohmic. An anneal treatment at a temperature of 850 ^{o}C for 30 sec. in N_2 ambient was performed in order to form the ohmic contacts. The Ti anneal forms TiN interfacial layer resulting in N vacancies in the GaN thereby causing an increase in the donor concentration.

Sheet resistance of about 3.38 x 10^6 Ω/sq, contact resistance of about 12 x 10^3 Ω and contact resistivity value of 3 x 10^{-3} Ωcm^2 were extracted from the plot of total resistance as a function of the pad separation.

Current-voltage characteristics of the Ni/AlGaN/GaN rectifying contacts were plotted and analyzed. For the contact diodes where thermionic emission is the dominant current conduction mechanism, the current density can be expressed as [12]:

$$J = J_S[\exp(qV/kT) - 1], \text{ or } J \approx J_s \exp(qV/nkT) \text{ for } V >> 3kT/q, \quad (1)$$

where

$$J_s = A^* T^2 \exp\left(-\frac{q\Phi_b}{kT}\right), \quad (2)$$

and n is the ideality factor given by

$$n = \frac{q}{kT}\frac{\delta V}{\delta \ln J}, \quad (3)$$

T is the temperature, V the applied voltage, and A^* the effective Richardson constant. The theoretical value of the effective Richardson constant is given by [13]:

$$A^* = \frac{2\pi q m^* k^2}{h^3}, \quad (4)$$

where h is the Planck's constant and m^*, the effective mass. For a given "x", the effective mass is estimated by linear interpolation from the theoretical value $m^* = 0.35m_o$ for AlN and $m^* = 0.22m_o$ for GaN [14, 15].

A linear plot of the I-V characteristics obtained from Ni/AlGaN/GaN Schottky contacts for various diameters showed a turn-on voltage between 2.3 and 2.7 V. The 400 μm device indicated a reverse leakage current of 1.6×10^{-11} A/cm^2 at –2.0 V, respectively.

Semilogarithmic plot of the forward characteristics of the contacts, as shown in Figure 6 exhibited a linear region with an ideality factor ~1.0, indicating that current conduction is dominated by thermionic emission. Calculated ideality factors and barrier height using equations 3 and 4 are values are summarized in Table 1.

Table 1. Ideality factors and barrier heights

Schottky Contact, μm	Reverse current I_R, at –2V, A/cm^2	Ideality factor, n	Barrier Height, Φ_b, eV
100	9.8×10^{-13}	1.0	1.0
200	7.2×10^{-13}	1.0	1.0
300	2.18×10^{-12}	1.0	1.0
400	1.6×10^{-11}	1.0	0.8

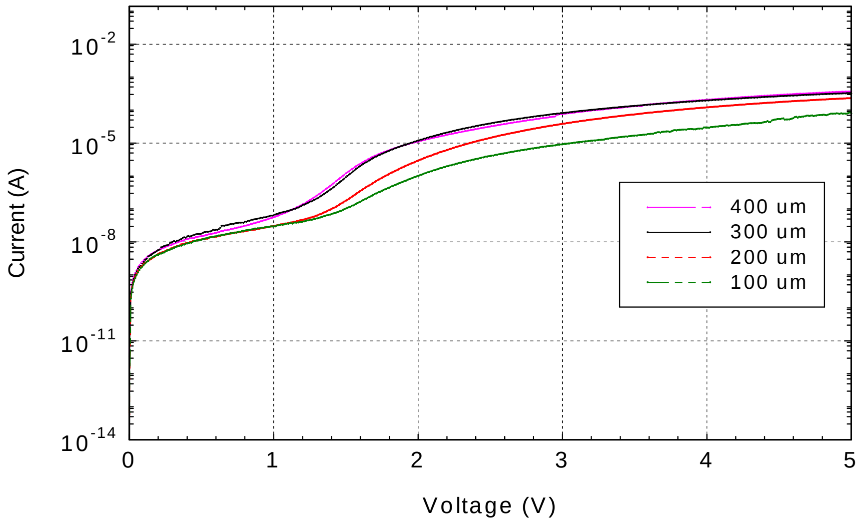

Figure 3. Semilogarithmic plot of the forward characteristics of Ni/AlGaN/GaN Schottky diodes

Capacitance – voltage (C – V) characteristics of the Schottky contacts

Capacitance-voltage measurements were obtained for the Ni/AlGaN/GaN rectifying diodes using an HP4284 LCR meter with 5 mV peak-to-peak voltages at a frequency of 1 MHz. Results obtained are shown in Figure 4. These C-V plots were used for the determination of conduction band discontinuity, polarization charge density, sheet carrier concentration and apparent carrier distribution profile at the AlGaN/GaN interface.

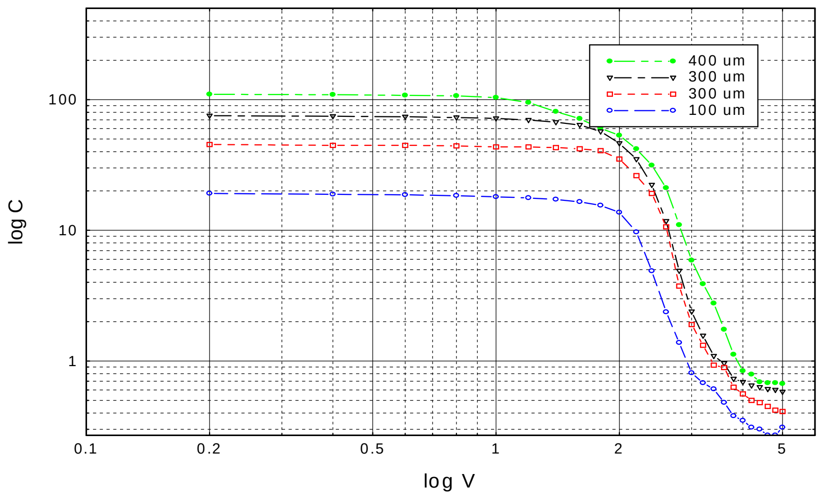

Figure 4. Capacitance - voltage plot for Ni/AlGaN/GaN rectifying contacts

The capacitance of a Schottky contact is given by [13]:

$$\frac{C}{A} = \sqrt{\frac{q\varepsilon_0\varepsilon(x)N_B}{2}}\left(V_{bi} \pm V - \frac{2kT}{q}\right)^{-1/2} \quad (5)$$

$$= \left(\frac{q\varepsilon_0 \varepsilon(x) N_B}{2V_{bi} \pm V - \frac{2kT}{q}} \right)^{1/2} ,$$

(6)

where V_{bi} is the built in potential, A, the area of the Schottky contacts, N_B, the background doping concentration. Equation 6 can be rewritten as

$$\left(\frac{C}{A}\right)^2 = \left(\frac{q\varepsilon_0 \varepsilon(x) N_B}{2\left(V_{bi} \pm V - \frac{2kT}{q}\right)} \right),$$

or

$$\left(\frac{A}{C}\right)^2 = \frac{2(V_{bi} \pm V - 2kT/q)}{q\varepsilon_0 \varepsilon(x) N_B} .$$

(7)

A plot of the inverse capacitance square ($1/C^2$) versus reverse bias voltage (V) is shown in Figure 8. The straight line in Figure 5 is given by:

$$\frac{1}{C^2} = \frac{2V}{q\varepsilon_0 \varepsilon(x) N_B A^2} + \frac{2V_{bi} - 2kT/q}{q\varepsilon_0 \varepsilon(x) A^2} .$$

(8)

The slope of the plot of $/C^2$ vs. V is given by:

$$slope = \frac{2}{q\varepsilon_0 \varepsilon(x) A^2 N_B} .$$

(9)

From the graph in Figure 6, the built-in potential, depletion width, apparent carrier concentration and sheet carrier concentration can be determined. The apparent carrier distribution n^* is given by [16]

$$n^* = N_B = \frac{2}{q\varepsilon_0 \varepsilon(x) A^2 slope} . \quad (10)$$

The depletion width, *w* is given by:

$$w = \frac{\varepsilon_0 \varepsilon(x) A}{C} = x_p + x_n , \quad (11)$$

where,

$$x_p = \left(\frac{2\varepsilon_0 \varepsilon(x) N_D (V_{bi} - V)}{qN_A (N_A + N_D)} \right)^{1/2} , \quad (12)$$

$$x_n = \left(\frac{2\varepsilon_0 \varepsilon(x) N_A (V_{bi} - V)}{qN_D (N_A + N_D)} \right)^{1/2} . \quad (13)$$

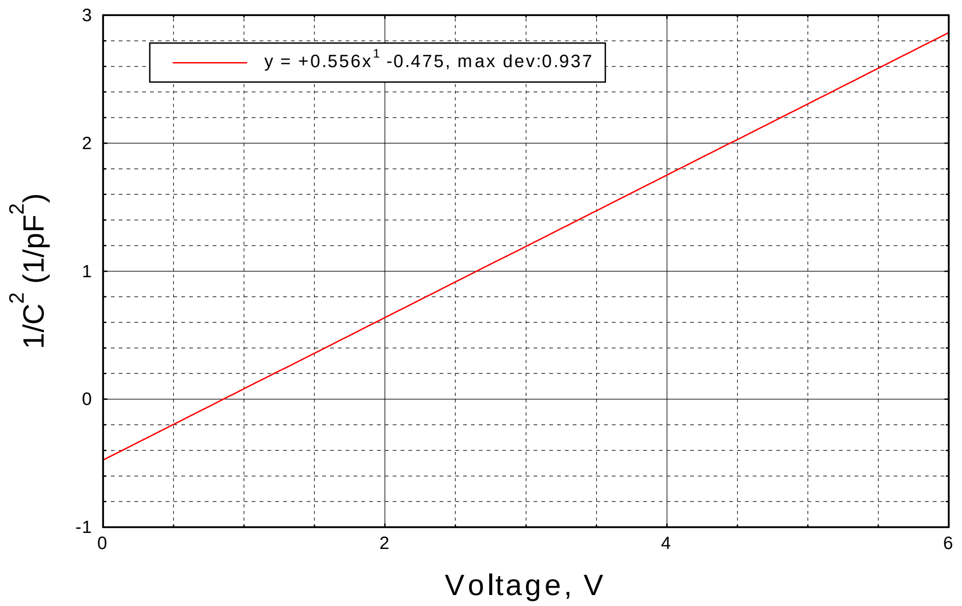

Figure 5. $1/C^2$ vs. V plot for 400 μm rectifying contact

For n-n unipolar heterostructure it was assumed that

$N_{AlGaN} = N_{GaN} = N$ and

$$w = \left(\frac{\varepsilon_0 \varepsilon(x)(V_{bi} - V)}{qN} \right)^{1/2} . \tag{14}$$

Current-voltage data of circular gate, π-gate, fatFET HEMT and Schottky diode have been collected with an HP4155A and plotted. With gate voltage, V_G from 0 to –4 at a step of –0.4 V and gate-to-drain voltage of up to 50 V, a drain current greater than 4.3 mA was obtained. For an n-channel mode transistor, a negative potential on the gate is required to turn the transistor channel off. A plot of the drain current as a function of drain voltage is shown in Figure 6. The I-V curves show a linear region where the drain current varies linearly with the applied grain voltage. This region is also known as the ohmic region (with $V_{ds} << V_{d,sat}$). The HFET devices have typical I-V characteristics for GaN as they exhibit some high field effect at the larger gate voltages. From the plots in Figure 10, transconductance and drift mobility values were estimated. At both high and low frequencies, the output drain current of a transistor is characterized by a current generator $g_m \times V_{gs}$, in parallel with the output conductance g_d [14, 15]. The transconductance g_m in a device is given by:

$$g_m = \frac{\partial I_D}{\partial V_{GS}} \bigg|_{V_{ds}} \approx \frac{\Delta i_d}{\Delta V_{GS}} \tag{15}$$

$$= \frac{qw}{l} \int_b^a \mu_d(x) n(x) dx \tag{16}$$

where $\mu_d(x)$ is the drift mobility at a depth x and n(x) is the carrier concentration, w the width and l the length of the channel.

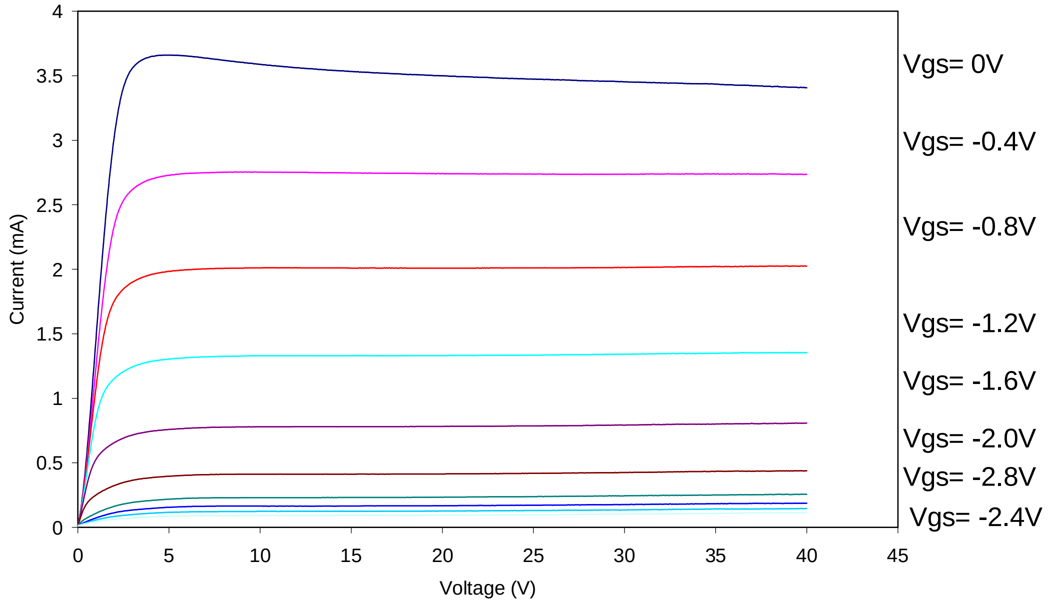

Figure 6. I_D vs. V_D characteristics of AlGaN/GaN HFET (10 µm)

Transconductance can also be given by:

$$g_m = \frac{qw}{l}\mu_d(x_0)n(x_0)V_{dd}\left(\frac{R_c}{R_T}\right)^2\left(\frac{\partial x_0}{-\partial v_{gg}}\right) \qquad (17)$$

where R_C is the channel resistance and R_T is the total resistance. From above relationships, transconductance of ~10 – 25 mS were obtained for the curves that exhibited a low field effect. The threshold voltage of -2.97 V was extracted. The average carrier concentration over a thickness of ≈ 2.3 $\times 10^{-8}$cm was determined to be n ≈ 8.5 $\times 10^{18}$cm^{-3}. A drift mobility of approximately 511 cm^2/Vs was estimated.

IV. CONCLUSION

Field effect transistors were fabricated on MBE grown films of $Al_{0.2}Ga_{0.8}N$/GaN heterostructure. A specific contact resistance of 1.33 × 10^{-2} Ω.cm^2 and a sheet resistance of 5.49 × 10^3 Ω/cm^2 was obtained for sputter deposited TLM pads which consisted Ni/Au (200/1500 Å) for p-AlGaN and Ti/Au (200/1500 Å) AlGaN/GaN. The contact resistance was high, but that was expected as the substrate was undoped. However, the sheet resistance was three orders of magnitude lower than the results reporter by Awaah for the same material system [10].

Rectifying contacts were obtained by depositing Ni (1500 Å) on the n-GaN. Ideality factors extracted from the current – voltage measurements were ~1.0, indicating that thermionic emission was the dominant transport mechanism. A barrier height of ~0.9 eV was determined for the Ni/n-GaN rectifying contact from I-V measurements. Analysis of C-V characteristics yielded an apparent carrier concentration of 1.02 × 10^{17} cm^{-3} and a sheet carrier concentration of 9.08 × 10^{11} cm^{-2}. These values are in good agreement with those reported by other researchers and the manufacturer of the substrate.

Fabricated AlGaN/GaN HFET devices exhibited transistor behavior with transconductance values ranging from 1.22 to 9.3 mS/mm. The threshold voltage was -2.97 V and a channel mobility of 484 cm^2 /V·s was obtained from the calculated transconductance. The n-GaN MESFETs fabricated on anneal treated substrates yielded transconductance values between 0.05 and 0.13 mS/mm. These devices achieved low saturation currents but no cut-off.

REFERENCES

[1] S. Nakamura and S.F. Chichibu, 2000. Introduction to Nitride Semiconductor Blue laser and Light Emitting Diodes, CRC press, Boca Raton.

[2] K. Linthicum, "GaN Overview", www.nitronex.com/education/ganOverview.pdf.
T.W. Staley and R.J. Matyi, 1997. "A Statistical Method for the Fitting of Double Crystal X-ray Rocking Curves", J. Appl. Crystallography, vol. 30, p. 368

[3] J. D. Brown, R. Borges, E. Piner, A. Vescan, S. Singhal, R. Therrien, 2002. "AlGaN/GaN HFETs fabricated on 100-mm GaN on silicon (111) Substrates", Solid State Electronics, vol. 46, pp.1535-1539.

[4] U. K. Mishra, P. Parikh, and Y. Feng Wu, 2002. "AlGaN/GaN HEMTs- An Overview of Device Operation and Applications", Proceedings of the IEEE, vol. 90, no. 6, p. 1022.

[5] W. Lu, V. Kumar, E. Piner, and I. Adesida, 2003. "DC, RF, and microwave noise performance of AlGaN/GaN field effect transistors dependence of aluminum concentration," IEEE Trans. Electron Devices, vol. 50, pp. 1069-1074.

[6] J. A. Smart, A. T. Schremer, N. G. Weimann, O. Ambacher, L. F. Eastman, and J. R. Shealy, 1999. "Growth of piezoelectric HEMT structures on sapphire and silicon carbide applying insulating AlGaN nucleation layer", Appl. Phys. Lett., vol 75, p. 388.

[7] M. A. Khan, Q. Chen, M. S. Shur, B. T. McDermott, J. A. Higgins, J. Burm, W. J. Schaff, and L. F. Eastman, 1996. "CW Operation of Short-Channel GaN/AlGaN Doped Channel Heterostructure Field Effect Transistors at 10 GHz and 15 GHz", IEEE Electron Device Lett., vol. 17, no. 12, pp. 584-585.

[8] R. Gaska, Q. Chen, J. Yang, A. Osinsky, M. A. Khan, and M. S. Shur, 1997. "High-Temperature Performance of AlGaN/GaN HFET's on SiC Substrates", IEEE Electron Device Lett., vol. 18, no. 10, pp. 492-494.

[10] A. Dabiram, 2005. SVT Associate (private communication).

[11] H.-Ki Kim, T-Y. Seong, I. Adesida, C. W. Tang, K. M. Lau. 2004. "Low-resistance Pt/Pd/Au ohmic contacts to p-type AlGaN", Appl. Phys. Lett., vol. 84, p. 10.

[12] A. M. Crowley and S. M. Sze. 1965. Surface States and Barrier Heights of Metal- Semiconductor Systems. J. Appl. Phys., vol. 36, p. 3212 Interscience, NY.

[13] S. M. Sze, 1981.Physics of Semiconductor Devices, John Wiley & Son.

[14] B. L. Anderson, and R. L. Anderson, 2005. Fundamentals of Semiconductor Devices, McGraw Hill.

[15] R. A. Pucel, and C. F. Krumm, 1974. "Simple method of measuring drift-mobility profiles in thin semiconductor films", Electronics Lett., vol. 12, no. 10, p. 240.